Quantitative Finance

ISSN: (Print) (Online) Journal homepage: https://www.tandfonline.com/loi/rquf20

Characterizing financial crises using high-frequency data

Mardi Dungey, Jet Holloway, Abdullah Yalaman & Wenying Yao

To cite this article: Mardi Dungey, Jet Holloway, Abdullah Yalaman & Wenying Yao (2022) Characterizing financial crises using high-frequency data, Quantitative Finance, 22:4, 743-760, DOI: 10.1080/14697688.2022.2027504

To link to this article: https://doi.org/10.1080/14697688.2022.2027504

Quantitative Finance, 2022
Vol. 22, No. 4, 743–760, https://doi.org/10.1080/14697688.2022.2027504

Characterizing financial crises using high-frequency data

MARDI DUNGEY†‡§, JET HOLLOWAY†, ABDULLAH YALAMAN *§¶ and WENYING YAO‖

†Department of Business and Economics, University of Tasmania, Hobart, Australia
‡Centre for Financial Analysis and Policy, University of Cambridge, Cambridge, UK
§Centre for Applied Macroeconomic Analysis, The Australian National University, Canberra, Australia
¶Department of Business Administration, Eskisehir Osmangazi University, Eskisehir, Turkey
‖Department of Economics, Deakin University, Burwood, Australia

(*Received 25 February 2021; accepted 3 January 2022; published online 11 February 2022*)

Recent advances in high-frequency financial econometrics enable us to characterize which components of the data generating processes change in crisis, and which do not. This paper introduces a new statistic which captures large discontinuities in the composition of a given price series. Monte Carlo simulations suggest that this statistic is useful in characterizing the tail behavior across different sample periods. An application to US Treasury market provides evidence consistent with identifying periods of stress via flight-to-cash behavior which results in increased abrupt price falls at the short end of the term structure and decreased negative price jumps at the long end.

Keywords: High-frequency data; Tail behavior; Financial crisis; US Treasury markets

JEL Classifications: C58, G01, G12

1. Introduction

The behavior of asset returns differs between a crisis and a non-crisis period in a number of ways. The stylized facts for returns in crisis period are that they are more volatile with large negative extreme values, often negatively skewed and display excess kurtosis compared with non-crisis periods. These distinctive features have been attributed to factors such as idiosyncratic shocks, the transmission of shocks from other markets, and changes in market conditions.† Crises are often characterized as 'fast and furious' (see Kaminsky *et al.* 2003). Given these observations, there is a surprisingly small existing literature on characterizing crises or contagion using high-frequency data; this very recent literature includes Black *et al.* (2012), Aït-Sahalia *et al.* (2015), Bollerslev *et al.* (2016), Alexeev *et al.* (2017), and Yao *et al.* (2020).‡

This paper examines changes in the high-frequency data generating process across crisis and non-crisis periods, we use an extension and application of the tools proposed in Aït-Sahalia and Jacod (2012a), which in turn summarizes the developments in Aït-Sahalia and Jacod (2009a, 2009b, 2010, 2011).§ Using these tools we show that the flight-to-cash hypothesis provides a useful means of identifying stress across the term structure of the US Treasury market. In doing so, this paper makes a number of contributions. The main contribution of the paper is the empirical insights regarding market stress in the Treasury market that can be gleaned from the differential behavior of the battery of tests in the Treasury price process before and during the crisis. In detail, we first introduce a new statistic which particularly captures the tail behavior of a given time series. We show that variations of this statistic are useful in characterizing the changing tail activities between two periods. Second, we use the set of high-frequency spectrum statistics to compare financial market data across different sample periods and characterize the US Treasury market using these innovative

*Corresponding author. Email: abdullahy@ogu.edu.tr, abdullah.yalaman@gmail.com

† For example almost all existing models of the transmission of crises through contagion can be characterized in this way. See the overview of modeling frameworks in Dungey *et al.* (2005).

‡ Although Pukthuanthong and Roll (2015) use the jumps technology developed for high-frequency data, they apply it to daily data.

§ A closely related statistic is the activity signature function proposed by Todorov and Tauchen (2010).

tools. The empirical analysis suggests that the most identifiable change in a crisis is contained in the tail observations, including potentially asymmetric changes in the positive and negative tails, consistent with the flight-to-cash hypothesis.

While our high-frequency data results show that the features which distinguish crisis from non-crisis periods are contained in the tail distributions, none of the statistics proposed within the Aït-Sahalia and Jacod framework emphasizes this part of the distribution. Therefore, we propose new measures which extend the spectrum statistics in Aït-Sahalia and Jacod (2012a) to tail behavior, which are found useful in characterizing crisis and non-crisis periods in the data. As the newly proposed statistics do not have tractable theoretical properties, we construct a simulation exercise to demonstrate its finite sample performance.

The paper also devises a new means of presenting the statistical results on the suite of statistics developed to characterize high-frequency data, which greatly aid in comparing sample periods. The Aït-Sahalia and Jacod framework uses two-dimensional distribution plots of multiple test statistics constructed on sub-samples of large data sets across a range of parameter calibrations. These visual tools pool statistics calculated using different power p and different sampling frequencies, with the grave disadvantage that the asymptotic limits of the test statistics are dependent on both the power and sampling frequency. We use the simulation experiment to demonstrate how this strategy can bias our perception of the data characteristics. We extend the visual representation to three dimensions to overcome this, in the sense that it takes into account the impact of power, p, and assess for a fixed sampling frequency. We simulate a number of standard models to show how the statistics behave in both two and three dimensions, revealing further refinements about the data generating mechanism.

To illustrate the use of these high-frequency statistics in characterizing the difference between non-crisis and crisis periods, we apply the set of statistics to the secondary trading in US Treasuries on the Cantor–Fitzgerald platform during the financial crisis period from July 2007 to December 2008, compared with a pre-crisis period from July 2004 to July 2007. We find clear evidence that the returns on 2, 5, 10 and 30-year bonds retain a Brownian motion component and the presence of jumps across non-crisis and crisis periods. The crisis period is distinguished by a decreased identification of jump activity. Additionally, there is evidence of behaviors consistent with the flight-to-cash hypothesis where investors reduce demand for long maturities (so that yields are unlikely to fall abruptly) and increase demand for short maturities (yields are more likely to fall abruptly).

The remainder of this paper is organized as follows. Section 2 outlines the framework suggested for characterizing high-frequency data drawing on the papers by Aït-Sahalia and Jacod (2009a, 2009b, 2010, 2011). It then constructs the new statistic S_{TI} which captures the tail behavior of returns. Section 3 shows a number of problems which may arise in using the existing representations of these statistics implemented in Aït-Sahalia and Jacod (2012a) when comparing data from non-crisis and crisis period. We design a simulation study and propose a different representation of the information which takes into account a further dimension of the parameter values. This information is used to evaluate the limiting values of S_{TI} with respect to different choices of parameters. Section 4 provides the application to US Treasury markets over the financial crisis period of 2007–2008, and shows statistically discernible changes between non-crisis and crisis periods, in particular, evidence of differing behavior at the short and long end of the yield curve. Section 5 concludes.

2. Measures of high-frequency market characteristics

Following Aït-Sahalia and Jacod (2012a), assume that the process characterizing the log-price for an individual asset in continuous time, denoted as X_t, is described by a semimartingale process of the form

$$X_t = X_0 + \underbrace{\int_0^t b_s \, \mathrm{d}s}_{\text{drift}} + \underbrace{\int_0^t \sigma_s \, \mathrm{d}W}_{\text{continuous component}} + \underbrace{\int_0^t \int_{[|x|\le\varepsilon]} x(\mu - \nu)(\mathrm{d}s, \mathrm{d}x)}_{\text{small jumps}} + \underbrace{\int_0^t \int_{[|x|>\varepsilon]} x \, \mu(\mathrm{d}s, \mathrm{d}x)}_{\text{large jumps}}, \tag{1}$$

where X_0 is a possibly non-zero mean, W denotes a standard Brownian motion, and b_s and σ_s measure the time-varying drift and volatility, respectively. For the discontinuous component of X_t, x represents the size of the jump, and the jump measure μ of X_t has a measurable compensator is the Levy measure ν. The last two terms in equation (1) represent first, possibly infinite many small jumps with jump size bounded by a chosen threshold ε which can be arbitrarily small, and second, a finite number of large jumps whose sizes exceed the threshold. The literature refers to these two components as 'infinite activity' and 'finite activity', respectively.

The first step in characterizing the data is to decide which of the components given in equation (1) are useful in describing the particular data series of interest. A given series may be comprised of a pure jump process, not requiring the continuous component, or a purely continuous process with no jumps, or contain some mixture of these.† Denote the size of the jump at time s by $\Delta X_s = X_s - X_{s-}$. Given a time interval $[0, T]$, the power variations of the true data generating process (DGP) (1) provide useful tools:

$$V(p) = \int_0^T |\sigma_s|^p \, \mathrm{d}s, \quad \text{and} \quad J(p) = \sum_{s \le T} |\Delta X_s|^p, \quad p > 0, \tag{2}$$

where in the case of $p = 2$, the terms in equation (2) are the two component of the quadratic variation of X_t on $[0, T]$:

$$[X_t, X_t]_{[0,T]} = \int_0^T |\sigma_s|^2 \, \mathrm{d}s + \sum_{s \le T} |\Delta X_s|^2 = V(2) + J(2). \tag{3}$$

In practice we don't usually have continuous record of price series, but work with equally spaced transaction data, using a

† The activity signature function of Todorov and Tauchen (2010) examines the same decomposition.

discretized form of equation (1). Given a fixed time interval $[0, T]$, we denote the log return by

$$\Delta_i^n X = X_{i\Delta_n} - X_{(i-1)\Delta_n}, \quad \text{for } i = 1, 2, \ldots, \lfloor T/\Delta_n \rfloor, \tag{4}$$

where Δ_n is the equi-distant time interval between successive X_t over the period $[0, T]$. Thus, there are $\lfloor T/\Delta_n \rfloor$ observations for a fixed T, where $\lfloor \cdot \rfloor$ denotes its integer part.

2.1. *Characterizing high-frequency returns*

In a series of papers, Aït-Sahalia and Jacod (2009a, 2009b, 2010, 2011) propose several statistics constructed using the discretely observed price series in (4) to determine which components of process (1) are present in a given asset price series. Consider the truncated power variation of the following form:

$$B(p, u_n, \Delta_n) = \sum_{i=1}^{\lfloor T/\Delta_n \rfloor} |\Delta_i^n X|^p \mathbb{1}_{\{|\Delta_i^n X| \le u_n\}}, \tag{5}$$

where u_n is the truncation level, and $\mathbb{1}$ is the indicator function such that $\mathbb{1}_{\{|\Delta_i^n X| \le u_n\}} = 1$ if and only if $|\Delta_i^n X| \le u_n$, and 0 otherwise. There are three parameters in the power variation specification of (5) available to examine different components of the price process; namely the power p, truncation level u_n, and the sampling frequency Δ_n.

Varying the power, p, usefully isolates either the continuous or jump component of process (1). When $p < 2$ the continuous Brownian component will dominate in (5), and the jump component will dominate if $p > 2$. In the commonly used realized variance measure, $RV = \sum_{i=1}^{\lfloor T/\Delta_n \rfloor} |\Delta_i^n X|^2$, the power $p = 2$ retains both continuous and jump components. The truncation level u_n can at maximum be infinity, in which case equation (5) becomes $B(p, \infty, \Delta_n) = \sum_{i=1}^{\lfloor T/\Delta_n \rfloor} |\Delta_i^n X|^p$. Sometimes $u_n \to 0$ is required in order for the statistics to converge to a proper limit. This is usually achieved by the following condition

$$u_n = \alpha \Delta_n^{\varpi}, \quad \text{where } \varpi \in (0, \tfrac{1}{2}), \text{ and } \alpha > 0 \text{ for } \Delta_n \to 0. \tag{6}$$

The value of α is generally set to be some multiple of the standard deviation of the Brownian component in the literature (Aït-Sahalia and Jacod 2012a), and $\varpi = 0.49$. Lastly, we may vary the sampling frequency by choosing an integer $k > 1$, in which case we use $B(p, u_n, k\Delta_n)$ to denote the case where lower sampling frequency $k\Delta_n$ is used to construct statistics (5).

The convenience of the measures given in equation (5) is that the behavior of a given series can be characterized by examining the effects of changing power, p, truncation level, u_n and sampling frequency ratio, k. Aït-Sahalia and Jacod (2012a) summarize a set of statistics which use these principles to test for: the presence of jumps, the presence of the Brownian motion, and whether the jumps have finite or infinite activity.† We present these test statistics below, and explain why and how we extend this set of measures to incorporate a new statistic to capture tail behavior.

There are three test statistics proposed by Aït-Sahalia and Jacod (2009b, 2011, 2010):

$$S_J(p, k, \Delta_n) = \frac{B(p, \infty, k\Delta_n)}{B(p, \infty, \Delta_n)}, \quad \text{with } p > 2 \text{ and } k \ge 2, \tag{7}$$

$$S_{FA}(p, u_n, k, \Delta_n) = \frac{B(p, u_n, k\Delta_n)}{B(p, u_n, \Delta_n)}, \quad \text{with } p > 2,\ k \ge 2 \text{ and } u_n \text{ satisfies (6)}, \tag{8}$$

$$S_W(p, u_n, k, \Delta_n) = \frac{B(p, u_n, \Delta_n)}{B(p, u_n, k\Delta_n)}, \quad \text{with } \beta < p < 2,\ k \ge 2 \text{ and } u_n \text{ satisfies (6)}, \tag{9}$$

where $\beta \in (0, 2)$ in (9) is the Blumenthal–Getoor index that measures the degree of jump activity.‡ These statistics identify the existence of different components in X_t according to:

(a) S_J converges to 1 when there are jumps (either finite or infinite activity) in X_t, and converges to $k^{p/2-1} > 1$ when X_t is purely a continuous Brownian process.
(b) S_{FA} converges to 1 when X_t contains jumps infinite activity, and converges to $k^{p/2-1} > 1$ when X_t has finitely many jumps and a Brownian component.
(c) S_W converges to 1 when X_t contains jumps infinite activity but no Brownian component, and converges to $k^{p/2-1}$ when X_t has a continuous Brownian component.

The contribution of this paper is to distinguish data from crisis and non-crisis samples via the characterization of the composition of asset returns provided by the statistics described above. However, it is well known that returns in crisis periods are more volatile, with large negative extreme values, and are often negatively skewed with excess kurtosis compared with their non-crisis counterparts. This motivates an extension of the suite of statistics to include an analogous specification focused on the tails of the distribution of asset returns. It complements the set of statistics proposed by Aït-Sahalia and Jacod (2009b, 2010, 2011) in the sense that it focuses on the large extreme observations in asset returns.

2.2. *The tail behavior of the distribution*

The Aït-Sahalia and Jacod (2012a) statistics cover the case of the whole distribution, S_J, and the truncated distribution, S_{FA} and S_W. To fill the missing section of the distribution we establish a new analogous statistic to examine the behavior of the tails of the distribution alone.

† Aït-Sahalia and Jacod (2009a) also include tests for infinite activity and no Brownian motion, but as they are not germane to the application here and thus omitted from our discussion.

‡ In practice, the degree of jump activity, β, needs to be estimated from the data. See Aït-Sahalia and Jacod (2009a), Aït-Sahalia and Jacod (2012b) for estimators of β which are based on the same series of truncated statistics. We use the estimator proposed in Aït-Sahalia and Jacod (2009a) to estimate β in the empirical application in Section 4.

Denote the upper truncated power variation by

$$U(p, u_n, \Delta_n) = \sum_{i=1}^{\lfloor T/\Delta_n \rfloor} |\Delta_i^n X|^p \mathbb{1}_{\{|\Delta_i^n X| > u_n\}}, \tag{10}$$

clearly $U(p, u_n, \Delta_n) = B(p, \infty, \Delta_n) - B(p, u_n, \Delta_n)$. Aït-Sahalia and Jacod (2010) and Aït-Sahalia and Jacod (2012a) also use $U(p, u_n, \Delta_n)$ to test the null hypothesis of no Brownian motion by setting $p = 0$, which effectively counts the number of large jumps, as $U(p, u_n, \Delta_n)$ retains only the finitely many large price movements as $\Delta_n \to 0$. We construct the statistic that captures the large jumps in X_t in particular,

$$S_{TI}(p > 2, u_n, k \geq 2, \Delta_n) = \frac{U(p, u_n, k\Delta_n)}{U(p, u_n, \Delta_n)} \tag{11}$$

detects the tail intensity of X_t, where $p > 2$, $k \geq 2$ and u_n satisfies condition (6). $U(p, u_n, \Delta_n)$ is always dominated by the jump components of the model regardless of whether the Brownian component is present or not.

An advantage of examining the tails of the distribution alone is that asymmetry can be easily accommodated. Bae *et al.* (2003) provide some empirical examples where large positive and large negative returns are not equally contagious. Recent studies on jump behaviors during crisis periods also find asymmetry in the tail distribution during period of market distress (Black *et al.* 2012, Alexeev *et al.* 2019). Denote

$$U^+(p, u_n, \Delta_n) = \sum_{i=1}^{\lfloor T/\Delta_n \rfloor} |\Delta_i^n X|^p \mathbb{1}_{\{\Delta_i^n X > u_n\}},$$

$$U^-(p, u_n, \Delta_n) = \sum_{i=1}^{\lfloor T/\Delta_n \rfloor} |\Delta_i^n X|^p \mathbb{1}_{\{\Delta_i^n X < -u_n\}}.$$

Then the statistics for positive and negative tail intensity are defined as follows:

$$S_{TI}^+ (p > 2, u_n, k \geq 2, \Delta_n) = \frac{U^+(p, u_n, k\Delta_n)}{U^+(p, u_n, \Delta_n)}, \tag{12}$$

$$S_{TI}^- (p > 2, u_n, k \geq 2, \Delta_n) = \frac{U^-(p, u_n, k\Delta_n)}{U^-(p, u_n, \Delta_n)}. \tag{13}$$

Unfortunately, although both components of $U(p, u_n, \Delta_n)$, $B(p, \infty, \Delta_n)$ and $B(p, u_n, \Delta_n)$, are analytically tractable, their combination in the form of our proposed statistic is not. Consequently, we turn to simulations to demonstrate the properties of all four statistics, S_J, S_W, S_{FA} and S_{TI} under a number of plausible DGPs.

2.3. *Distinguishing crisis periods*

This paper specifically considers how these statistics for high-frequency financial returns described above may differ between non-crisis and crisis periods. In this way, we are able to pin down the important components in financial returns, which in turn allows us to link more clearly with the literature on crisis transmission. In particular, if the characterization of jumps or tail behavior change, then this links strongly to the literature on non-linear transmission mechanisms which single out large or atypical observations as the key to understanding crises, as for example in the outlier based approach of Bae *et al.* (2003), Boyson *et al.* (2010), quantile approaches in Baur and Schulze (2005), Caporin *et al.* (2018) and jumps approach of Aït-Sahalia *et al.* (2015). On the other hand, if the Brownian motion or finite jump properties of the data change, this supports alterations of the fundamental process, such as the latent factor model approaches of Billio and Caporin (2010), Fry *et al.* (2010), Dungey *et al.* (2015) or the copula-based approaches of Busetti and Harvey (2011), Rodriguez (2007).

We approach this problem in two ways. The first is to compare the distribution of statistics suggested by Aït-Sahalia and Jacod (2012a) as described in the previous sections for non-crisis and crisis periods, and formally test whether they are significantly different. The distribution of each statistic is constructed for subsamples at a variety of power p and sampling frequencies k. Following Aït-Sahalia and Jacod (2012a), concatenating the generated statistics by power and sampling frequency forms a histogram of the test statistic for the asset return under consideration. This is then used to determine whether the statistic supports the null hypothesis or otherwise. The equality of the empirical distributions for the two sample periods is tested using a Kolmogorov–Smirnov test.

However, concatenating the test statistics calculated using different powers and sampling frequencies may not be desirable. In some cases, the resulting test statistics will produce outcomes which are rather difficult to interpret. More fundamentally, the representation may mislead the researcher. Consider, for example, the case for S_J when $p = 2.2$. The value associated with H_0 (jumps) is 1, and the value associated with H_1 (no jumps) is $k^{0.1}$ which, for the cases $k = \{2, 3\}$, is $\{1.07, 1.12\}$. However, if $p = 4$, under H_0 we have $S_J = 1$, and under H_1 for $k = \{2, 3\}$, S_J takes the values $\{2, 3\}$, respectively. This means for small values of p, S_J will have mass concentrated around 1 even when H_0 is false. When concatenating the calculated S_J over all values of p, this will tend to make the histograms appear to support H_0.

As will be shown in the empirical example, this problem is most apparent for the S_J statistic. In the next section, we use simulations to address the extent of these problems using the S_J statistic as the exemplar. In particular, we examine the distribution of S_J, given different values of the power p, while controlling k at a single value. In this way, we avoid mixing the results in a counter-intuitive manner.

The second aspect of this problem is addressed using the proposed S_{TI} statistic and its variations for asymmetry S_{TI}^+ and S_{TI}^-. By comparing the distributions of S_{TI} for crisis and non-crisis periods, we are able to detect whether the tail activity of the underlying price process changes during the crisis period. We start with the concatenated statistics over a range of values for the power p and frequency k, and then plot the distribution of S_{TI} as a function of p while k is kept fixed. However, while examining the distribution of S_{TI}, rather than letting the sampling interval Δ_n approach 0, we fix $\Delta_n = 5$ and obtain the simulated distribution of S_{TI} under different circumstances. This is the most realistic situation in practice, because letting Δ_n tend to 0 is not achievable. More importantly, researchers

often choose to work with lower sampling frequencies to avoid market microstructure noise (see, for example, Andersen *et al.* 2007) and the 5 minute frequency is highly used in practical applications (see also the discussion in Dungey *et al.* (2009b) for evidence on the sampling frequency choices for US Treasury market data). The separation between positive and negative tail intensities enables us to investigate the prevalence of positive and negative jumps during the two subperiods, respectively. This type of asymmetric behavior has been documented by Jiang *et al.* (2011), Bjursell *et al.* (2013) and Black *et al.* (2012), who find that in the non-crisis period, the number of positive jumps is usually far higher than the number of negative jumps. Bae *et al.* (2003) draw a similar conclusion that large positive and large negative returns are not equally contagious. This shift in the intensity of tail activity between non-crisis and crisis periods may be useful as a signal in detecting crisis stress.

3. Simulation study

We use a series of Monte Carlo simulations to investigate the finite sample properties of the test statistics outlined in Section 2. We consider four cases as the baseline processes: Brownian motion, a regime switching Brownian motion, a skewed distribution based on Azzalini (1985),† and a stochastic volatility model based on Nelson (1990).‡ The regime switching Brownian process has 10 potential regimes, and 5 orders of magnitude between the volatility of the least and most volatile regimes with random switching.§ Each of these baseline models is simulated for the cases of no jumps, finitely many small jumps and finitely many large jumps. Jumps arrive according to a Poisson process, and when an interval is selected to be a jump, its return is multiplied by a scaling factor. For small jumps, returns are multiplied by 3, and for large jumps, the returns are multiplied by 6. Thus, at any given point in time, the size of potential jumps scales with the volatility of the process.

The simulation parameters are calibrated to a liquid equity, the same as those used in Aït-Sahalia and Jacod (2009a), which in turn are based on the estimates of the Heston model for the S&P500 data in Aït-Sahalia and Kimmel (2007). The sampling frequency used in their calibration (approximately every 5 seconds) is far in excess of the liquidity of the data samples in the applications of this paper, so our calibrations correspond to 114 observations of 5-minute intervals per day.¶ For each process specification we simulate 100 observations, each of which is a price history containing 7 years of 5-minute data (252 trading days in each year). This choice of 1764 trading days per price history is chosen according to the Treasury bond data we have in the empirical application. The parameter for the Poisson process is set so that the expected number of jumps is 700 in each realization of 7 years of price history, hence the Poisson parameter is 2.778.

The parameters for the statistics are set to be consistent with those used in Aït-Sahalia and Jacod (2012a). We fix $k = 2$, and calculate all of the statistics for 40 different values of p in the range of $[2.1, 6]$ with step size 0.1. We then generate histograms for these statistics that are aggregated over the different values of p, and the three-dimensional simulated distributions at each different values of p. The truncation parameter α in implementing S_{TI} is set to be a multiple of the standard deviation of the continuous component of the process over a 5-minute interval. This standard deviation is estimated using the truncated power variation from equation (5) with $p = 2$. In the simulation, we set $\alpha = 3 \cdot \sqrt{B(2, u_n, \Delta_n)}$ and $\varpi = 0.49$ for S_{TI}.

3.1. *Exploring the role of p in the distributions*

Figure 1 plots the two-dimensional simulated distribution of the statistics S_J for each scenario. The simulated density in percentage terms is on the vertical axis, and the value of the S_J statistic is on the horizontal axis, as suggested by Aït-Sahalia and Jacod (2012a). Figure 2 plots the three-dimensional simulated distribution of S_J, over a range of different values of the power p. Figure 2(a) shows that in the case of Brownian motion with no jumps, the mass is heavily centered around the theoretical value $k^{p/2-1}$. It is also apparent that as p increases, the distribution becomes more diffuse, although the average value of S_J remains at $k^{p/2-1}$. By comparing to the corresponding two dimensional chart in figure 1, it is evident that larger values of p result in increasing values of S_J. When we plot S_J on the two-dimensional simulated distribution, regardless of what value p takes, a lot of mass is close to 1 due to the small values of p. Overall, the distribution is very dispersed within the interval $[1, 4]$. Thus, the choice of p at which to evaluate the statistic will make a difference to how well we are able to identify different outcomes from figure 1.

Figure 2(b,c) reveals that the addition of small jumps to Brownian motion results in a deviation of the simulated distribution from the theoretical value 1, while in the case of large jumps the mass is much closer to 1 at all values of p examined. All of the simulated distributions become more diffuse as p increases. The same panels of figure 1 show that in the presence of small jumps, the greatest mass is located at roughly

† A continuous random variable Z with probability density function $f(z) = 2\phi(z)\Phi(\alpha z)$, where $\phi(z) = \exp(\frac{-z^2}{2})/\sqrt{2\pi}$ is a normal density, $\Phi(\alpha z) = \int_{-\infty}^{\alpha z} \phi(t)$ is a normal distribution function, α is the shape parameter that affects the skewness of the random variable. In the simulation the shape parameter is set to be $\alpha = 4$, implying a skewness of 0.78, which is consistent with the skewness observed in financial returns data (see for example Fry *et al.* 2010).

‡ In order to produce the main features of stochastic volatility model, we generate instantaneous log-returns by the continuous-time martingale: $\mathrm{d}p(t) = \sigma(t)\mathrm{d}W_p(t)$, where $W_p(t)$ denotes a standard Wiener process, and $\sigma(t)$ is given by a separate continuous time diffusion process. For, a diffusion limit of the GARCH(1,1) process is specified for $\sigma(t)$:

$$\mathrm{d}\sigma^2(t) = \theta(\omega - \sigma^2(t))\mathrm{d}t + (2\lambda\theta)^{1/2}\sigma^2(t)\mathrm{d}W_\sigma(t),$$

where $\omega > 0$, $\theta > 0$, $0 < \lambda < 1$, and the Wiener processes, $W_p(t)$ and $W_\sigma(t)$, are independent. The parameters values $\omega = 0.636$, $\theta = 0.035$, and $\lambda = 0.296$ are chosen according to Andersen and Bollerslev (1998).

§ This is motivated by the literature which proposes a regime switching framework during crises, such as Akay *et al.* (2013).

¶ Trading for the secondary US Treasury bond market is open for 9.5 hours per day from 8:00 am to 5:30 pm, which amounts to 114 observations with 5-minute intervals.

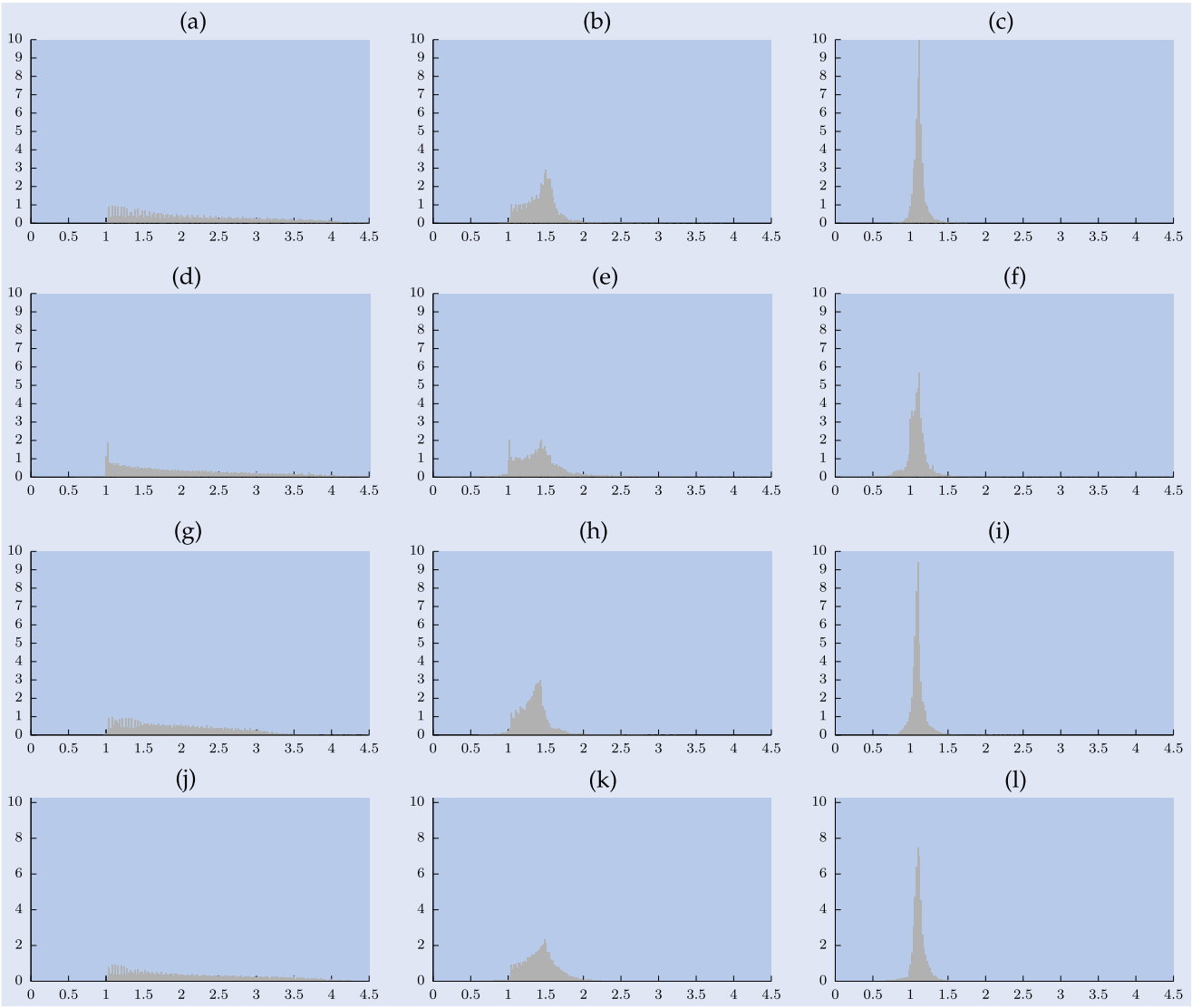

Figure 1. Simulated distributions (probability density functions) of S_J (two-dimensional representation). $2.1 \leq p \leq 6, k = 2$. (a) Brownian motion. (b) Brownian motion with jumps. (c) Brownian motion with large jumps. (d) Brownian motion with regimes. (e) Brownian motion with regimes and jumps. (f) Brownian motion with regimes and large jumps. (g) Skewed normal distribution. (h) Skewed normal distribution with jumps. (i) Skewed normal distribution with large jumps. (j) Stochastic volatility model. (k) Stochastic volatility model with jumps and (l) Stochastic volatility model with large jumps.

1.6, whereas the distribution is much more concentrated at values close to 1 when there are large jumps. The difficulties of visually detecting small jumps are clearly evident. Compared with figure 2, the two-dimensional plots in figure 1 are much less informative and conclusive.

In Panel (d) of the regime switching model with no jumps, the simulated distribution looks very similar to the simple Brownian motion shown in Panel (a). However, when small jumps are introduced into the DGP, the distribution of the statistic S_J in figure 2 becomes more diffuse, especially for large values of p. In general, the simulated S_J statistic tracks its asymptotic limiting values quite well in all three situations, although large jumps are more easily detectable than small jumps. The skewed distributions in the third row of figures 1 and 2 have slightly differently distributed mass to the previous cases. It produces more mass closer to $S_J = 1$ in the two-dimensional representation, and deviates from the theoretical values in the three-dimensional representation (figure 2(g)) when there are no jumps—an important consideration given that increased skewness is commonly associated with crisis periods (see Fry *et al.* 2010).

The stochastic volatility model produces similar two-dimensional distributions of S_J as the distribution from Brownian motion, as shown in the last row of figure 1. Figure 2(j,l) shows that its three-dimensional distribution tracks the theoretical limit fairly well in the case of no jumps or large jumps. However, in the case of small jumps, the three-dimensional distribution of S_J is more dispersed over the range between 1 and 2. This demonstrates better detection of small jumps in the stochastic volatility model than the previous cases.

If we use the two-dimensional representations in figure 1 to detect jumps, comparing the no jump representations between these experiments provides little visual difference. In the case of small jumps, regime switching is less likely to emphasize the presence of jumps, but skewness and stochastic volatility

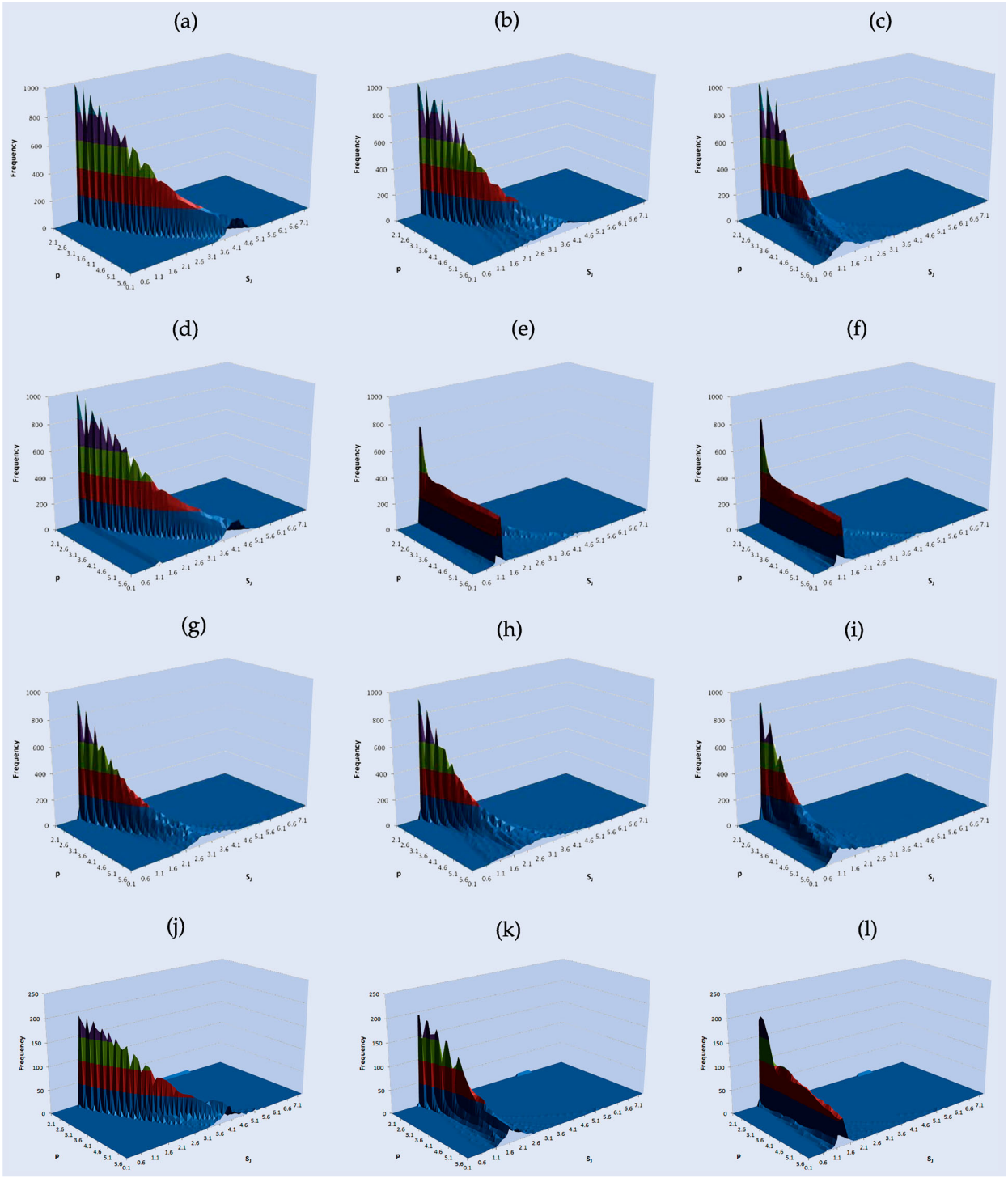

Figure 2. Simulated distribution of S_J as functions of p (three-dimensional representation). $2.1 \leq p \leq 6, k = 2$. (a) Brownian motion. (b) Brownian motion with jumps. (c) Brownian motion with large jumps. (d) Brownian motion with regimes. (e) Brownian motion with regimes and jumps. (f) Brownian motion with regimes and large jumps. (g) Skewed normal distribution. (h) Skewed normal distribution with jumps. (i) Skewed normal distribution with large jumps. (j) Stochastic volatility model. (k) Stochastic volatility model with jumps and (l) Stochastic volatility model with large jumps.

increase the mass of the distribution that is closer to 1. In the case of large jumps, all distributions exhibit a clustering around 1, although this is less pronounced in the case of regime switching model with large jumps. This evidence supports the contention that other features of the data may well be biasing our visual categorization of the process in the two-dimensional distributions, particularly in the presence of either skewness or changes in regime.

Overall, the comparison between figures 1 and 2 reveals the difficulty of using the two-dimensional distribution in figure 1 to test the presence of jumps visually. Especially when there are small jumps in the DGP, the values of S_J are not concentrated around $S_J = 1$. Figure 2 shows that this is because as p increases, the calculated S_J is more likely to obtain higher values, which in turn confound the evidence of jumps in the two-dimensional representation. Thus, figure 2

presents a refinement of the assessment tools by taking into account changes in the power p, and extending the representation to three dimensions while holding k fixed. Examining the distributions of S_J as functions of p provides distinguishable features for the visual inspection of small or large jumps. This is particularly true for large values of p, as the cases of no jumps, small jumps and large jumps lead to more distinct value ranges for the S_J statistic.

3.2. *The behavior of S_{TI}*

The two- and three-dimensional simulated distributions of S_{TI} are presented in figures 3 and 4, respectively. Panel (a) of Brownian motion with no jumps stands out in both figures, noticing the different scale on the y-axis in figure 4(a). When the underlying true DGP consists of a well-behaved Brownian motion, but does not contain a jump component, the value of S_{TI} statistic is strikingly high at above 6 consistently. Figure 4 indicates that the distribution in accordance to different values of p is quite dispersed compared with the distribution of S_J, but this does not affect the visual identification given the high median.

In the presence of jumps, figure 4(b,c) makes the distinction between small and large jumps very clear. Large jumps dominate $U(p, u_n, \Delta_n)$ for $p > 2$ at any sampling frequency, and hence the S_{TI} statistic is heavily centered around 1. When the jumps are smaller, values of S_{TI} are mostly above 1.5 across the whole range of p considered. These results offer a valid device to distinguish the cases of no jumps, small and large jumps, as the range of values that S_{TI} takes under these three situations rarely overlap. The advantage of the three-dimensional plots is manifest in figure 4. Although the confounding caused by different values of p has much less impact on the distribution of S_{TI} than the statistics examined in the previous sub-section, taking into account p provides much more informative guide in testing the existence of the jumps.

When we introduce the possibility of regime switching and skewness into the underlying DGP, the distribution of S_{TI}

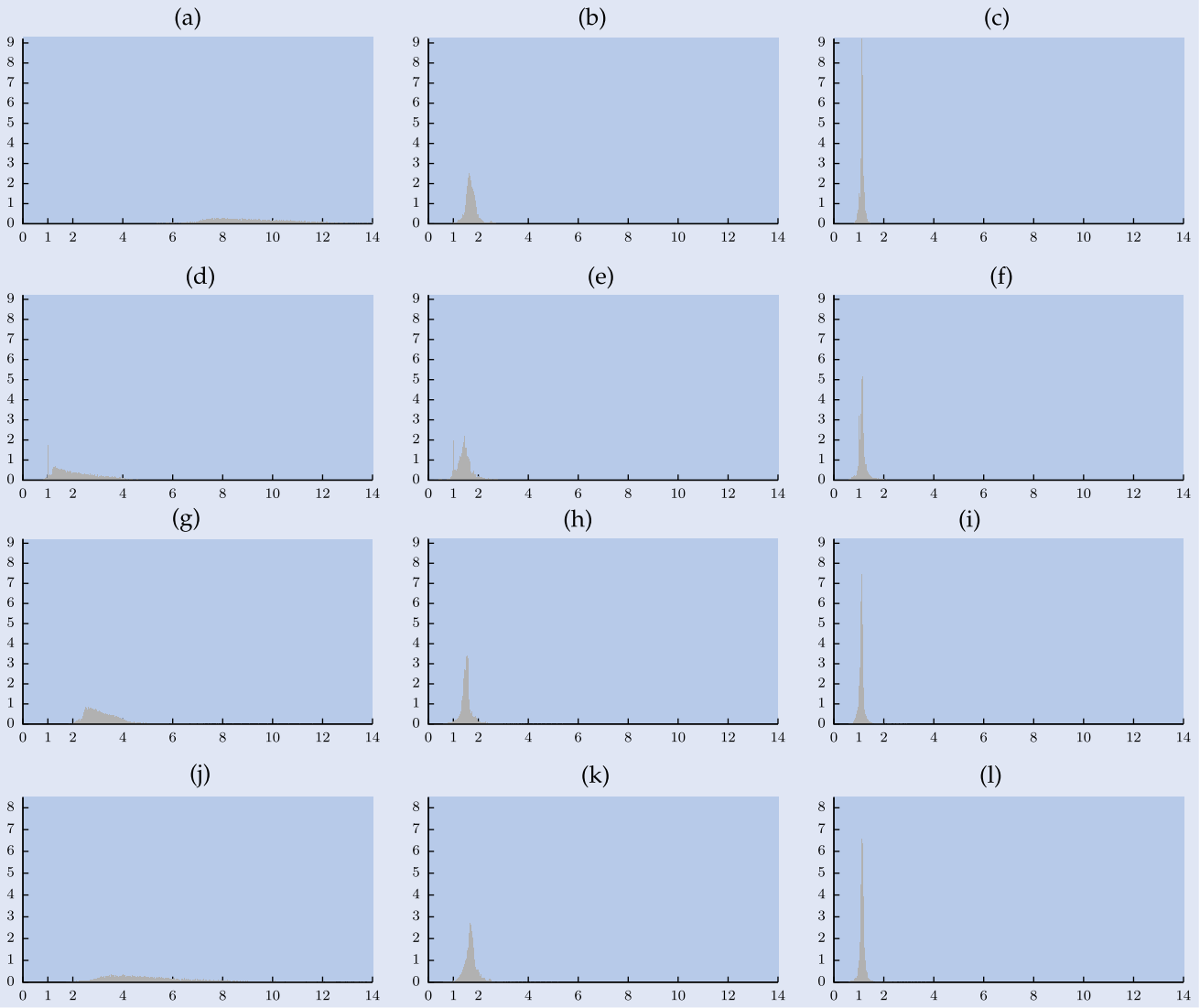

Figure 3. Simulated distributions (probability density functions) of S_{TI} (two-dimensional representation). $2.1 \leq p \leq 6$, $k = 2, \alpha = 3\sqrt{B(2, u_n, \Delta_n)}$. (a) Brownian motion. (b) Brownian motion with jumps. (c) Brownian motion with large jumps. (d) Brownian motion with regimes. (e) Brownian motion with regimes and jumps. (f) Brownian motion with regimes and large jumps. (g) Skewed normal distribution. (h) Skewed normal distribution with jumps. (i) Skewed normal distribution with large jumps. (j) Stochastic volatility model. (k) Stochastic volatility with jumps and (l) Stochastic volatility with large jumps.

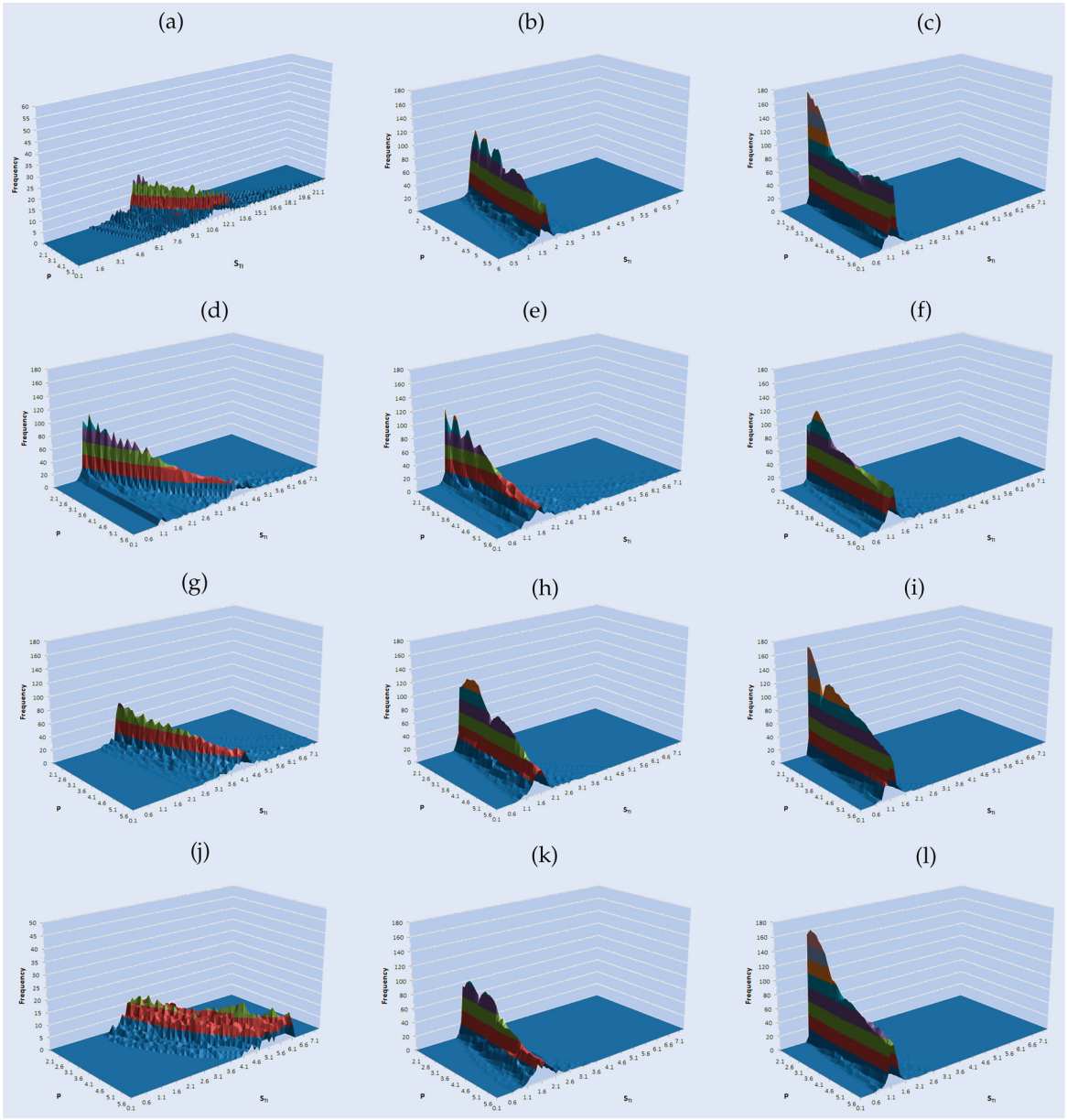

Figure 4. Simulated distribution of S_{TI} as functions of p (three-dimensional representation). $2.1 \leq p \leq 6, k = 2, \alpha = 3\sqrt{B(2, u_n, \Delta_n)}$. (a) Brownian motion. (b) Brownian motion with jumps. (c) Brownian motion with large jumps. (d) Brownian motion with regimes. (e) Brownian motion with regimes and jumps. (f) Brownian motion with regimes and large jumps. (g) Skewed normal distribution. (h) Skewed normal distribution with jumps. (i) Skewed normal distribution with large jumps. (j) Stochastic volatility model. (k) Stochastic volatility model with jumps and (l) Stochastic volatility model with large jumps.

deviates from the frictionless baseline scenario. Most evident are the cases with no jumps as shown in Panels (d) and (g) in figures 3 and 4. With regime switching the distribution of S_{TI} is very similar to the distribution of the S_J statistic shown in figure 2(d). The values of S_{TI} increase monotonically as we increase the power parameter p. A skewed distribution produces values that are strictly above 2, which provides a favorable tool in distinguishing jumps when the majority of the mass is heavily distributed around 1. The detection of small jumps becomes more difficult in the presence of regime switching or skewness. Under the regime switching model the distribution of S_{TI} quickly becomes diffuse as the value of p increases. With skewness a non-negligible proportion of the distribution mass is close to unity, which is commonly interpreted as a sign of large jumps.

The last row of figure 3 shows that two-dimensional distributions of S_{TI} in the stochastic volatility model is similar to those obtained for the Brownian motion case. The only difference is that in the case of no jump, the S_{TI} statistic usually takes a smaller value between 3 and 8. The three-dimensional representations for the stochastic volatility model shown in figure 2 are similar to the case of skewed normal distributions.

By design, the S_{TI} statistic emphasizes the extreme returns in the tails of the distribution. The simulation result above verifies the usefulness of S_{TI} in distinguishing the three cases in the underlying DGP: no jumps, small jumps and large jumps. Given the three-dimensional representation in figure 4, it is evident that S_{TI} produces distinct patterns as functions of p for different types of tail activities. More importantly, when the jumping behavior in the DGP changes, the values of S_{TI}

Table 1. Descriptive statistics of the 5-minute return in the pre-crisis period of July 1, 2004 to July 16, 2007 and crisis period of July 17, 2007 to December 31, 2008.

	Pre-crisis period				Crisis period				
	2-year	5-year	10-year	30-year	2-year	5-year	10-year	30-year	scale
Mean	−0.120	0.016	0.704	2.218	1.724	2.873	2.826	3.896	10^{-6}
St.D.	0.749	1.816	2.955	5.233	1.700	3.703	5.317	9.369	10^{-4}
Min.	−0.251	−0.580	−0.867	−2.161	−0.361	−0.757	−0.688	−1.290	10^{-2}
Max.	0.459	1.233	1.509	1.902	0.335	0.693	0.761	1.102	10^{-2}
Skew.	3.476	5.258	2.442	0.005	0.047	−0.067	−0.165	−0.247	
Kurt.	323.121	434.718	174.866	107.754	28.635	21.596	9.677	10.573	

reside in alternate regions with very few overlapping areas. Thus, considering the large body of evidence that information about crises and contagion is contained in the tail distributions of returns, S_{TI} seems to be a useful tool to add to the suite of characterizing statistics described in Aït-Sahalia and Jacod (2012a).

Another important observation from figure 4 is that higher values of power p can help the S_{TI} statistic better distinguish the cases of no jumps, small jumps and large jumps. This is particularly pronounced at the point where $p \in (4, 5)$, which is close to the suggested calibration value in Aït-Sahalia and Jacod (2009a). Higher values of p magnify the effect of jumps, as the upper truncated power variations retain only the jumps. Therefore, the effect of large p is more pronounced on the S_{TI} statistic than S_J.

4. Empirical results: the US Treasury market

The secondary market for US Treasuries is one of the largest individual asset markets in the world. At the end of our sample period in 2008, it recorded a turnover of over $US120 trillion per day. The majority of trade has migrated to two dominant electronic communication networks (ECNs) since the turn of the century, one now known as Cantor Fitzgerald (formerly known as BGCantor and eSpeed) and the other BrokerTec. The existing empirical evidence suggests that total turnover is reasonably evenly divided between them—Mizrach and Neely (2006) find approximately 40% of ECN turnover on BGCantor, but more recent comparisons in Jiang *et al.* (2011) and Dungey *et al.* (2009b) make it closer to 50% each. The US Treasury market played a key role in the flight to liquidity and quality, which occurred in the crisis of 2007–2008, as it did during the period of the Hong Kong dollar speculative double play, and the near collapse of the US-based hedge fund Long-Term Capital Management in August and September 1998 in Dungey *et al.* (2009a). The jump behavior of this market, and the associated futures market, has been documented in Dungey *et al.* (2009b), Lahaye *et al.* (2011), Jiang *et al.* (2011), Dungey and Hvozdyk (2012) and Bjursell *et al.* (2013).

In order to examine the differences between non-crisis and crisis period trading, we divide our total sample period of July 1, 2004 to December 31, 2008 into two subsamples: a calm period beginning with the upswing of interest rates from the previous US monetary policy cycle, and a crisis period beginning from July 17, 2007. The breakpoint between the pre-crisis and crisis periods is consistent with the first indications of troubles from hedge funds at Bear-Stearns and precedes the changes in policy at the European Central Bank on August 9, 2009. Both of these dates have been used to mark the start of the crisis elsewhere.† The data covers the main US trading hours from 8:00 am to 5:30 pm EST for the secondary trading in 2, 5, 10 and 30-year bonds.

4.1. *Characterization of pre-crisis and crisis periods*

Table 1 presents the descriptive statistics of the 5-minute returns during the pre-crisis and crisis periods.‡ We also plot the histogram of the return distributions in figure 5. The average returns are all very close to zero (note the scaling factor of 10^{-6}), but the standard deviations have increased for all maturities during the crisis period. Bonds with longer maturities also show higher variations. Interestingly, the pre-crisis sample is always more positively skewed than the crisis sample, especially for bonds with shorter maturities. This is also confirmed by the empirical distributions depicted in figure 5. The crisis sample, however, is almost symmetrically distributed, with the exception of the 30-year bond.

Figure 6 presents the daily realized variance calculated from 5-minute returns in each maturity throughout the sample period, and the summary statistics of the daily realized variances for the two subperiods are given in table 2. There is a clear increase in variance (and also covariance which is not reported here) for assets during the crisis period compared to the relatively tranquil non-crisis period. Large increases in realized variance occur in July–August 2007 around the beginning of the crisis, with greater rises in September–December 2008 during the period of the bankruptcy of Lehman Brothers, the rescue of AIG, collapse of Fannie Mae and Freddie Mac and numerous other instances of institutional stress. We also report the estimates obtained using realized kernel figure 7 as robustness check. They show very similar patterns to the realized variance depicted in figure 6.

† There are many chronologies of the crisis events of 2007–2008, including Rose and Spiegel (2012) and Bordo (2008).
‡ Aït-Sahalia and Jacod (2012a) emphasize that unequally spaced data would potentially be more informative but the theory is not yet available to fully account for the endogeneity issue (see Aït-Sahalia and Jacod 2012a, page 1013). Thus the models used in this paper only use regular sampling.

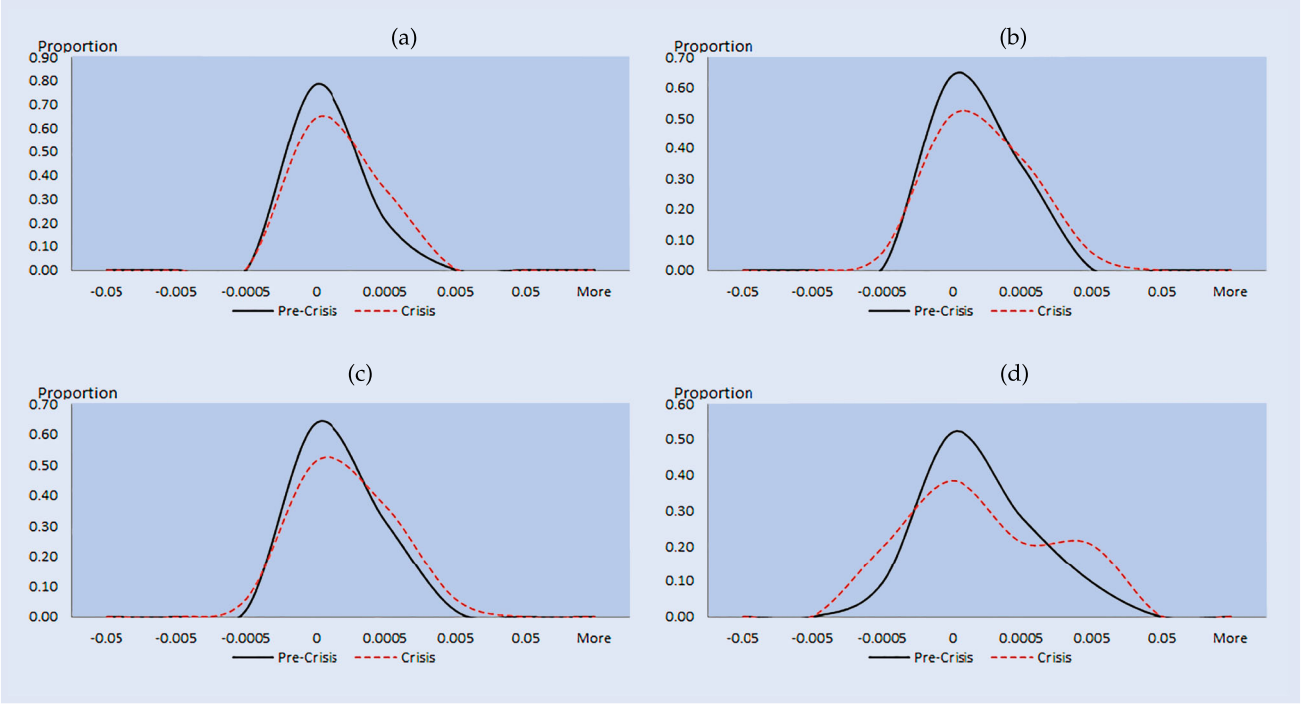

Figure 5. Empirical distributions of the 5-minute returns for US Treasury bonds in pre-crisis and crisis periods. (a) 2-year bond. (b) 5-year bond. (c) 10-year bond and (d) 30-year bond.

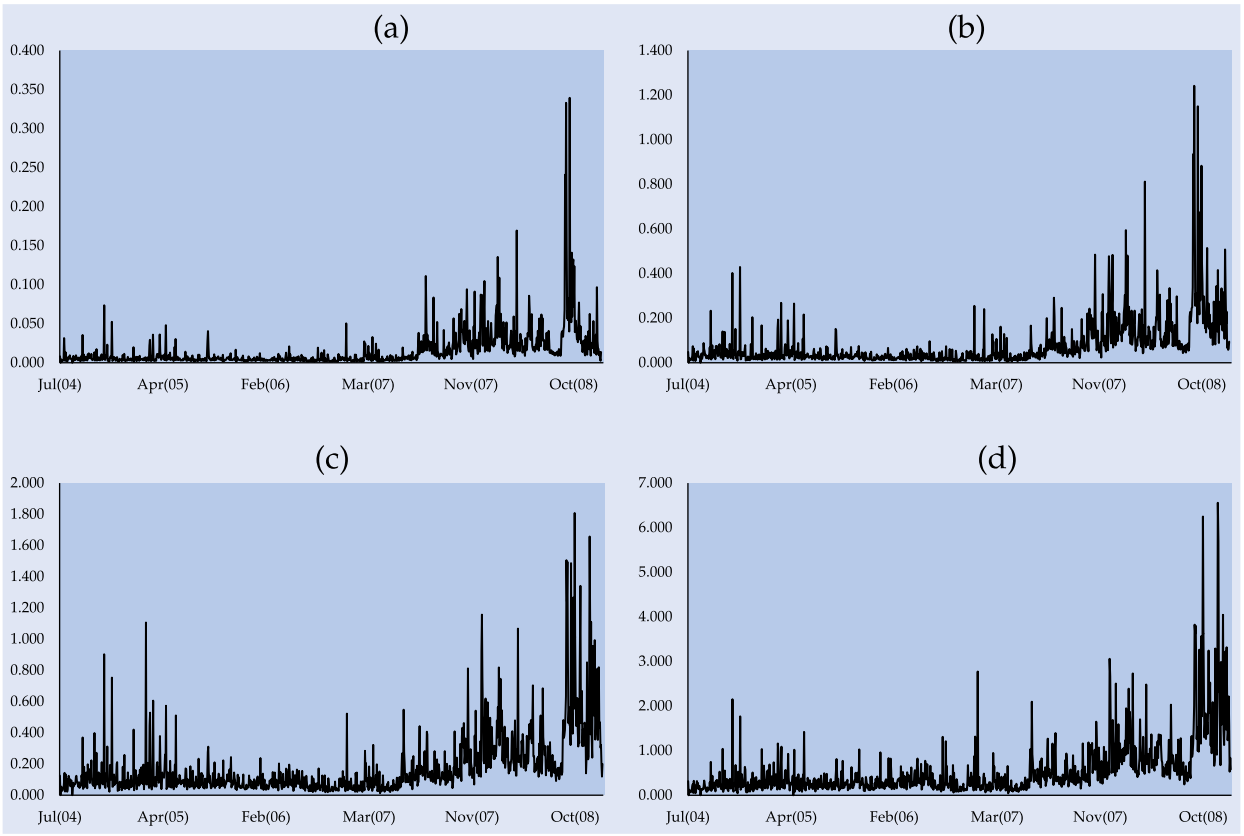

Figure 6. Realized variance of 2, 5, 10 and 30-year maturity US Treasury bonds. (a) 2-year bond. (b) 5-year bond. (c) 10-year bond and (d) 30-year bond.

Table 2. Descriptive statistics of the realized variance in the pre-crisis period of July 1, 2004 to July 16, 2007 and crisis period of July 17, 2007 to December 31, 2008.

	Pre-crisis period				Crisis period			
	2-year	5-year	10-year	30-year	2-year	5-year	10-year	30-year
Mean	0.006	0.034	0.095	0.295	0.033	0.154	0.322	1.001
St.D.	0.006	0.038	0.091	0.247	0.036	0.148	0.267	0.863
Min.	0.001	0.004	0.012	0.043	0.003	0.021	0.046	0.150
Max.	0.074	0.429	1.106	2.774	0.339	1.242	1.809	6.558

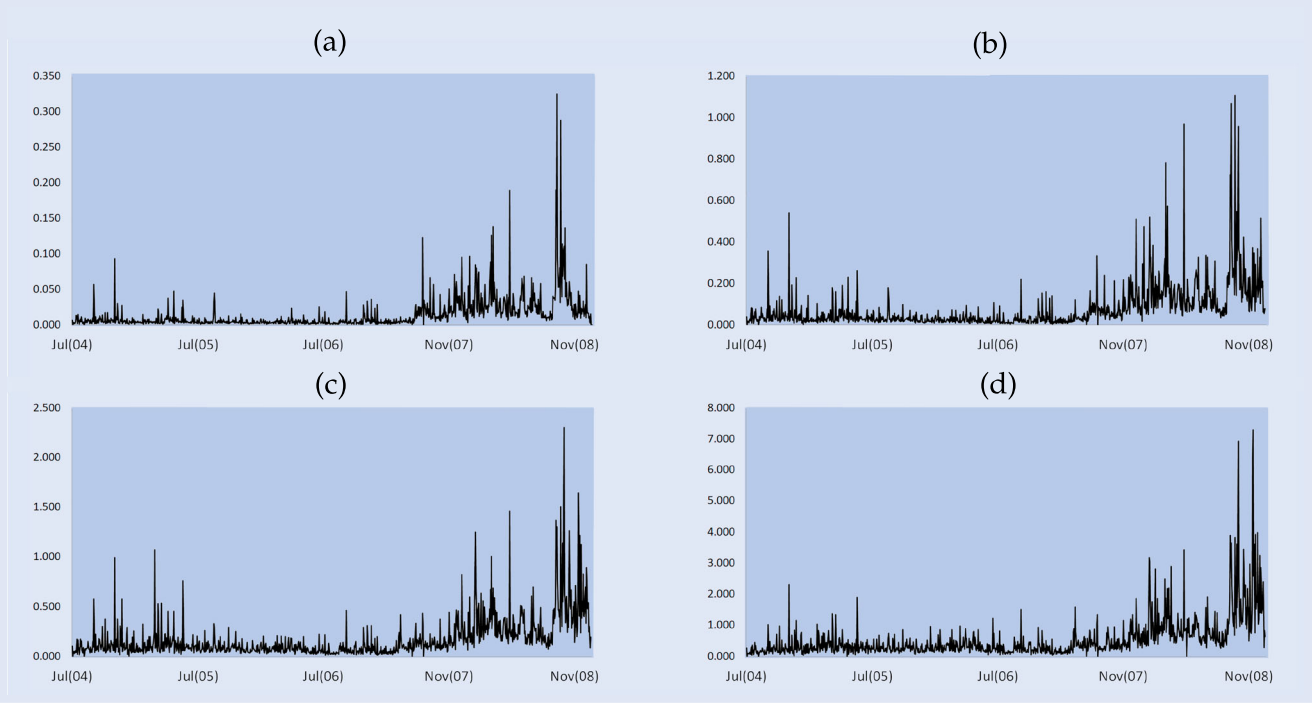

Figure 7. Realized Kernel variance (Bartlett kernel) of 2, 5, 10 and 30-year maturity US Treasury bonds. (a) 2-year bond. (b) 5-year bond. (c) 10-year bond and (d) 30-year bond.

4.1.1. Evidence for jumps: S_J. The empirical distributions of the test statistic for the presence of jumps S_J for the pre-crisis sample (solid line) and the crisis sample (dashed line) are shown in figure 8(a). The data are presented as yields, thus a positive jump represents a rise in yield, associated with a corresponding fall in the bond price. Each line represents the values obtained for S_J as p varies across $2.1 \leq p \leq 6.0$ in 0.1 increments and $k = 2, 3$ pooled for all maturities as suggested in Aït-Sahalia and Jacod (2012a). The median of the distribution is slightly larger than 1 for both crisis and non-crisis periods, which provides supporting evidence for jump activity.

Comparing the two-dimensional distributions for the two subsample periods, it is apparent that the mass of the

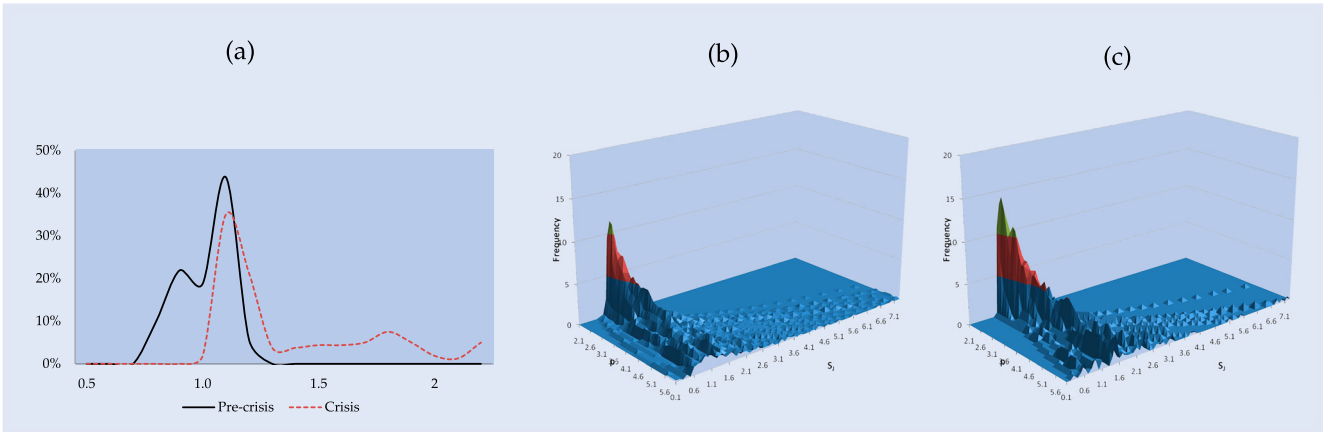

Figure 8. Empirical distributions of the S_J statistic for US Treasury bonds in pre-crisis and crisis periods ($2.1 \leq p \leq 6$, $k = 2, 3$). (a) Two-dimensional representation. (b) Three-dimensional representation (non-crisis period) and (c) Three-dimensional representation (crisis period).

Table 3. Kolmogorov–Smirnov test statistics for equality in two-dimensional cumulative density functions of the S_J, S_{FA}, S_W and S_{TI} between the pre-crisis (July 1, 2004 to July 16, 2007) and crisis (July 17, 2007 to December 31, 2008) subsamples.

	S_J	S_W	S_{FA}	S_{TI}	S_{TI}^+	S_{TI}^-
Test statistic	0.6625	0.1094	0.1656	0.7500	0.7813	0.2094
p-value	(0.0000)	(0.4072)	(0.0003)	(0.0000)	(0.0000)	(0.0000)

Table 4. The estimated degree of jump activity for the pre-crisis period of July 1, 2004 to July 16, 2007 and crisis period of July 17, 2007 to December 31, 2008.

	Pre-crisis period				Crisis period			
	2-year	5-year	10-year	30-year	2-year	5-year	10-year	30-year
Both tail	0.9989	1.0039	1.0005	1.0001	1.0021	1.0010	0.9998	1.0001
Left tail	0.9833	0,9630	0.9448	0.9414	1.0001	0.9842	1.0069	0.9889
Right tail	1.0156	1.0491	1.0605	1.0620	1.0041	1.0162	0.9923	1.0112

distribution has shifted to become right skewed during the crisis rather than left skewed in the pre-crisis period. The median of the distribution is slightly large than 1 for both non-crisis and crisis periods, which provides evidence supporting jump activity. However, while the crisis distribution has practically all of its mass above unity, the non-crisis distribution has a second mode to the left of $S_J = 1$. This suggests that during the crisis period jumps are more easily detected, whereas during pre-crisis period the jump evidence is mixed with microstructure noise.† A Kolmogorov–Smirnov test strongly rejects the null that the two subsample distributions are the same, as reported in table 3. This motivates us to examine these figures in three dimensions which take into account changes in the power p, similar to the presentation of the simulation results in Section 3.

The three-dimensional representations of the S_J statistic for the Treasury bonds during the non-crisis and crisis periods are presented in figure 8(b,c). For the three-dimensional plots, we use one month of high-frequency data as windows to calculate each statistic, in contrast to the two-dimensional plots where the entire (either pre-crisis or crisis) history per observation. This is mainly due to the fact that we need more observations in order to display reliable distributional features for each value of p, as we do not concatenate over different values of p in the three-dimensional plots. We also only use $k = 2$, so that for a given value of p there will only be one limiting value for the case of no jumps, namely $2^{p/2-1}$. Figure 8(b,c) shows that for small values of p, there is limited variation near the value of 1 around the median S_J. However, as p increases the mass quickly disperses, leaving much greater variance at higher p. The difference between pre-crisis and crisis distributions is unclear from the three-dimensional plot, which makes the distribution very uninformative. As p increases, there is increased uncertainty about comparisons across the two periods. The suggested value of $p = 4$ in Aït-Sahalia and Jacod (2009a) is unlikely to yield useful results here.

4.1.2. Evidence for Brownian motion: S_W. The statistic S_W requires that the power p satisfies $\beta < p < 2$, where β is the Blumenthal–Getoor index that measures the degree of jump activities. In any practical applications, the value β is unknown and needs to be estimated. We use the estimator proposed in Aït-Sahalia and Jacod (2009a), which is closely related to the upper truncation in (10) and hence the resulting S_{TI} statistic in (11). Denote

$$\widetilde{U}(\varpi, \alpha) = \sum_{i=1}^{\lfloor T/\Delta_n \rfloor} \mathbb{1}_{\{|\Delta_i^n X| > \alpha \Delta_n^{\varpi}\}}, \quad \varpi \in \left(0, \frac{1}{2}\right), \tag{14}$$

and recall that $u_n = \alpha \Delta_n^{\varpi}$ is the truncation threshold used in the S_W, S_{FA}, and S_{TI} statistics. We can think of $\widetilde{U}(\varpi, \alpha)$ in (14) as $U(p, u_n, \Delta_n)$ with power parameter $p = 0$, and hence only counts the number of returns that exceed the threshold $u_n = \alpha \Delta_n^{\varpi}$. Instead of varying power p and the sampling interval Δ_n, $\widetilde{U}(\varpi, \alpha)$ uses alternative values of the truncation threshold. Let $0 < \alpha < \alpha'$ be two constants, then

$$\hat{\beta} = \log\left(\frac{\widetilde{U}(\varpi, \alpha)}{\widetilde{U}(\varpi, \alpha')}\right) \cdot \frac{1}{\log(\alpha'/\alpha)} \tag{15}$$

provides a consistent estimator of β. We choose α so that $\widetilde{U}(\varpi, \alpha)$ retains 5% of the tail distribution of returns, and $\alpha' = 2\alpha$.

The estimated degree of jump activity using the bond data is presented in table 4. In addition to the original estimator (15) proposed in Aït-Sahalia and Jacod (2009a), we follow the construction of S_{TI}^+ and S_{TI}^- to calculate the jump activity estimator for the left tail and right tail separately. All estimates are around 1, indicating that the choice of power p for S_W should satisfy $p \geq 1$. The jump activity using both tails of the return distribution suggests an increased jump activity for short-term bonds during the crisis, but not for the long-term 10-year and 30-year bonds. A closer inspection of the left and right tails separately indicates that the changes in the degree of activity for negative jumps (left tail) has increased across all maturities, but decreased across all maturities for positive jumps (right tail).

Figure 9(a) plots the distribution of the S_W statistics calculated for two subsample periods for $1 \leq p \leq 1.75$ with increments of 0.05, and for $k = 2$, 3. The striking aspect of the figure is that the results clearly support the presence of Brownian motion in the data generating process, and the

† The theoretical limit of S_J is $1/k$ when additive noise dominates, is $1/\sqrt{k}$ when rounding error dominates. See Aït-Sahalia and Jacod (2012a) for details.

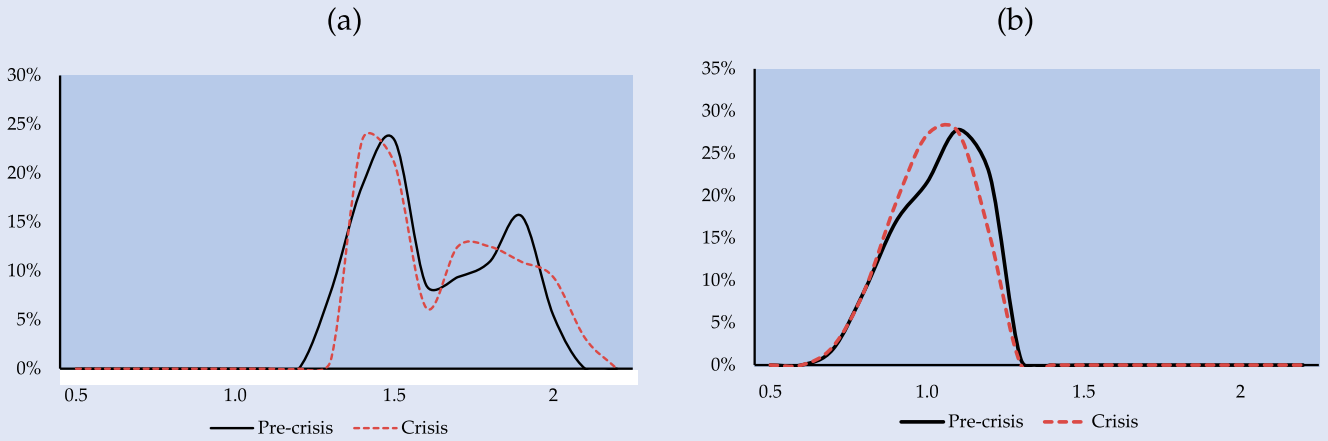

Figure 9. Two-dimensional representations of the S_W and S_{FA} statistics for US Treasury bonds in pre-crisis and crisis periods. (a) S_W, $1 \leq p \leq 1.75$, $k = 2, 3$ and (b) S_{FA}, $2.1 \leq p \leq 6$, $k = 2, 3$.

distribution hardly changes between the non-crisis and crisis samples. This is confirmed by the Kolmogorov–Smirnov test statistic reported in table 3. Thus the existence of the Brownian motion cannot be used to distinguish data from non-crisis and crisis periods.

4.1.3. Evidence for finite jump activity: S_{FA}. Prior to examining the S_{TI} statistic for tail behavior, we first calculate whether the jumps detected earlier have finite activity using the S_{FA} statistic. The empirical distribution of the test statistic for whether jump activity is finite, S_{FA}, is given in figure 9(b), where the statistics are calculated across all maturities for $2.1 \leq p \leq 6.0$ in 0.1 increments, $\alpha = 5$ and $k = 2, 3$.

The mass of the distribution covers the range from 0.5 to 1.5 but both the pre-crisis and crisis distributions are centered around 1, consistent with infinite jump activity. The distributions appear very similar in the two subsample periods, although the Kolmogorov–Smirnov test statistic in table 3 rejects the null that the two distributions are the same. The most visible difference between these two subsample distributions is that the pre-crisis data has a higher proportion of mass distributed at around 1.2 while the crisis data leans towards 1. Since values of S_{FA} calculated using different values of p are pooled together in the two-dimensional plot, it is difficult to classify whether values such as $S_{FA} = 1.2$ support finite or infinite jump activity.

4.2. Evidence for tail intensity: S_{TI}

The two-dimensional distributions of S_{TI}, S_{TI}^+ and S_{TI}^- are presented in figure 10. As in the cases for S_J and S_{FA}, we set $k = 2, 3$, and vary p across $2.1 \leq p \leq 6$ in increments of 0.1. We set $\alpha = 3$ in order to examine the tails of the distribution. The last three columns in table 3 suggest changes in their distributions from the pre-crisis to crisis periods. It is also clear that the figures look quite different in the two subsamples. There is greater certainty in distinguishing the presence of jumps from noise and small jumps. Figure 10(a) shows that values of S_{TI} are mostly around 1 during the pre-crisis period, but the mass has increased to higher values during crisis. This reveals that there is a decreased presence of large jumps during the crisis period.

Figure 10(b,c) plots the two-dimensional representation of S_{TI}^+ and S_{TI}^- for the positive and negative tail activities. There is strong evidence of large positive jumps during the pre-crisis period, but during the crisis period, the positive tail intensity tends to indicate small or no jump activity. Thus S_{TI}^+ provides useful information in distinguishing the crisis and non-crisis periods. In the case of negative tail activity, the distinction between the pre-crisis and crisis data is less pronounced than for the positive tail. Comparing figure 10(b,c), the statistics suggest that during the pre-crisis period there is more evidence for large positive jumps than for large negative jumps, but during the crisis period the negative jumps have greater mass around larger jumps than in the positive jumps case. Again, the Kolmogorov–Smirnov test reported in table 3 strongly rejects the equality of these two distributions, so we can conclude that changes in the tail behaviors at both ends may be useful in distinguishing crisis periods.

Reconciling the results on the intensity of jump activity using these tails with the existing literature is complicated by maturity structure and asset class. For example, Li *et al.*

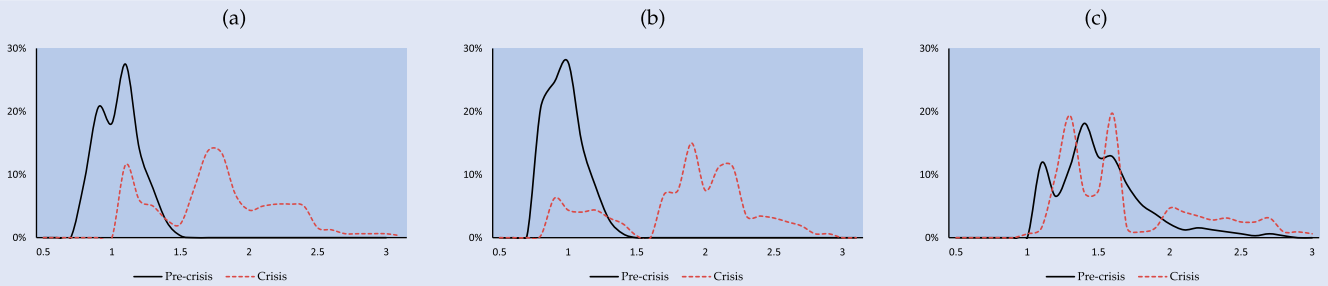

Figure 10. Two-dimensional representations of S_{TI}, S_{TI}^+ and S_{TI}^- statistics for US Treasury bonds in pre-crisis and crisis periods ($2.1 \leq p \leq 6$, $k = 2, 3$). (a) S_{TI}. (b) S_{TI}^+ and (c) S_{TI}^-.

(2017) and Alexeev *et al.* (2019) both find that the S&P500 index has the lowest number of jumps during crisis, particularly in 2008. Black *et al.* (2012) report that for the S&P500 index, the annual number of positive jumps usually exceeds the number of negative jumps, *except* during the crisis year of 2008, when positive and negative jump occurrence was approximately even. In an application to the US Treasuries market, Jiang *et al.* (2011) find that the number of positive jumps exceed negative ones for all maturities except the relatively illiquid 3-year note over a non-crisis sample of January 2004 to June 2007. In contrast, Bjursell *et al.* (2013) find more negative than positive jumps for 10-year and 30-year maturities during 2001–2004, which contains both the dot-com crisis and the subsequent recovery periods. Because the bond market has a number of roles to play during periods of stress, through both flight-to-safety and flight-to-cash effects, it is worth considering the evidence with respect to individual maturities.

4.3. Changing behavior in the crisis

There is a growing body of research investigating the changing behavior of financial asset prices using data observed at high frequency. For example, Alexeev *et al.* (2017) examine the changes in market beta during periods of stress and the role of firm characteristics in the Global Financial Crisis (GFC). Dungey *et al.* (2020) analyze eight Asian exchange rate series using the same set of statistics presented in our paper. They find that the discernible feature of crises comes from the jumps. Most of the literature develops high-frequency statistics to examine changes in comovements and shock transmission between assets during crisis. For example, Aït-Sahalia *et al.* (2015) consider financial contagion through the lens of mutually exciting Hawkes processes. Bormetti *et al.* (2015) and Calcagnile *et al.* (2018) provide clear evidence that a Poisson assumption for the extreme event behavior should be rejected in favor of an alternative based on self-exciting Hawkes processes. Aït-Sahalia and Xiu (2016) find an increase in volatility as well as comovements among different asset classes during the GFC. Dungey *et al.* (2018) identify that flight-to-safety from stock to gold occurs more often than flight-to-quality from stocks to bonds during crisis.

During periods of stress, increased volatility in other markets may prompt investors to turn to safer assets, such as bonds, inducing a drop in yield (or negative jump) across the term structure. At the same time, increased uncertainty around all longer-term prospects results in flight-to-cash, producing rising yields (positive jumps) in longer term maturities, and falling yields (negative jumps) at the short-end of the curve. We separate the bonds into different maturities (2, 5, 10 and 30 years), and plot the median values of the statistics S_{TI}, S_{TI}^{+} and S_{TI}^{-} as functions of p in figure 11. Each row in figure 11 represents one maturity, and the three columns are for S_{TI}, S_{TI}^{+} and S_{TI}^{-}, respectively.

The difference in jump prevalence between the non-crisis and crisis period is smallest at the short-end of the sample, as shown for the 2-year bond in figure 11(a)–(c). However, as p increases, it is possible to see a degree of divergence between the pre-crisis and crisis lines. In particular, figure 11(a,c), S_{TI}^{-} demonstrate that there is increased evidence for negative jumps as p increases, consistent with the hypothesized behavior in the presence of a flight-to-cash during crisis. In the middle of the term structure, for the 5-year bonds, the evidence is consistent with a lower jump intensity during the crisis than the non-crisis period.

At the long end of the maturity structure for 10-year and 30-year bonds, the statistics shown for figure 11(g–l) support fewer jumps in the crisis period. Moreover, in the negative tail during the crisis, figure 11(i,l) suggest a substantial reduction in the evidence for negative jumps compared with the non-crisis period. Coupled with the lack of evidence for divergence of the crisis and non-crisis periods with increasing p in the positive tail shown in figure 11(h), these results are also consistent with the flight-to-cash hypothesis. It appears that the flight-to-quality argument is outweighed in the empirical evidence by flight-to-cash concerns which result in increased desire to hold short-maturity Treasuries.

In summary, the values of S_{TI}, S_{TI}^{+} and S_{TI}^{-} lie in the interval $[1, 2]$ in most cases, and when plotting the statistics against p, most lines are relatively flat. In the simulated cases of no jumps discussed in Section 3.2, they all increase with p and are much larger than 1. Hence given the simulation results in figure 4, we conclude that US Treasury bonds have small to large jumps across different maturities. For the purpose of distinguishing crisis from non-crisis data, the distinctive features are the general reduction in evidence for jumps during periods of crisis compared with non-crisis samples, and in the bond markets the evidence that as p increases we are able to detect increasing divergence between the non-crisis and crisis samples consistent with increased demand for short-maturity securities (resulting in more occurrences of abrupt price declines) and decreased demand for long-maturity securities (resulting in fewer occurrences of abrupt price declines), consistent with existing evidence in lower frequency data on flight-to-cash during periods of financial stress.

5. Conclusion

The behavior of financial market data during periods of financial stress is of great practical importance to investors, analysts and policy makers alike. Crisis models often assume that some underlying data generating mechanism remains stable across both non-crisis and crisis periods, but is augmented by new or enhanced features during the crisis period. This paper develops a suite of tools, extending those proposed by Aït-Sahalia and Jacod (2009b, 2010, 2011), in order to examine which aspects of data generating mechanism remain stable, and which change during a crisis. This set of statistics is based on the behavior of the tails of the returns only, and is capable of treating left and right tails separately, to account for potentially changing skewness patterns identified in Fry *et al.* (2010).

Applying these statistics to data on US Treasury bonds data reveals that the evidences for Brownian motion and finite or infinite activity jumps are not significantly changed between a

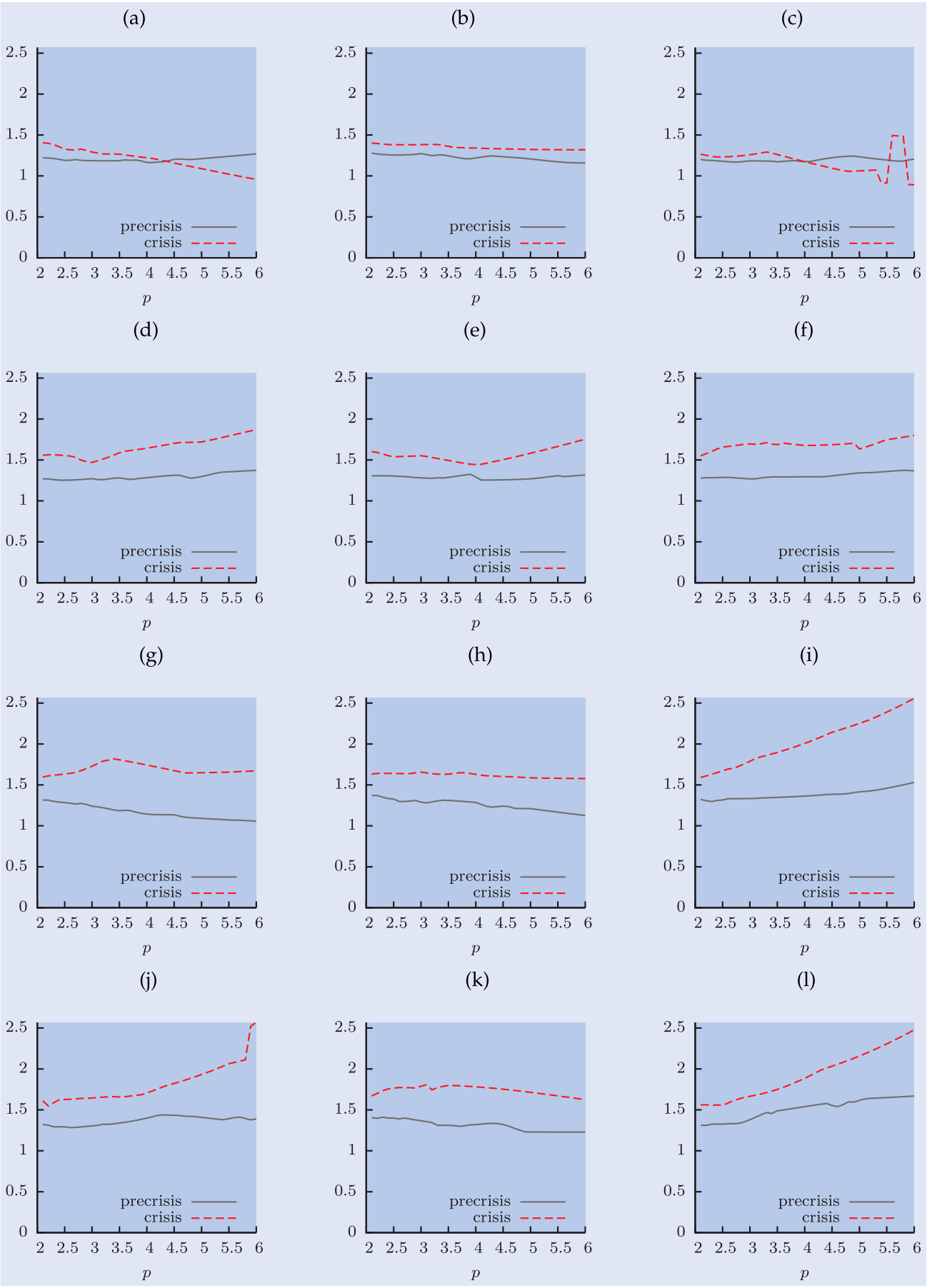

Figure 11. Three dimensional representations of the S_{TI}, S_{TI}^{+} and S_{TI}^{-} statistics for US Treasury bonds with separate maturities in pre-crisis and crisis periods ($2.1 \leq p \leq 6$ and $k = 2$). (a) S_{TI} for 2-year bond. (b) S_{TI}^{+} for 2-year bond. (c) S_{TI}^{-} for 2-year bond. (d) S_{TI} for 5-year bond. (e) S_{TI}^{+} for 5-year bond. (f) S_{TI}^{-} for 5-year bond. (g) S_{TI} for 10-year bond. (h) S_{TI}^{+} for 10-year bond. (i) S_{TI}^{-} for 10-year bond. (j) S_{TI} for 30-year bond. (k) S_{TI}^{+} for 30-year bond and (l) S_{TI}^{-} for 30-year bond.

pre-crisis period and the financial crisis of 2007–2008. However, the statistics concerning the presence of jumps differ. The difference between the two periods supports a greater ability to discern jump activity during the pre-crisis period, with the distribution of the jump statistic more concentrated around the critical value associated with jumps and also displaying right skewness. These findings are consistent with the features during periods of market stress identified by Dungey *et al.* (2020), which utilize the same set of statistics on eight Asian exchange rate series. Further, the results show a general decrease in the occurrence of jumps during crisis periods compared with non-crisis, and a pattern consistent with a slight increase in propensity for negative jumps in yield (that is increases in price) at the short end of the maturity and decreased propensity for negative jumps in yield (that is fewer increases in prices) at the long end of the maturity structure. These findings are consistent with flight-to-cash increasing the desirability of short maturity bonds during the crisis period.

Acknowledgments

Mardi Dungey passed away in January 2019, shortly after this paper was completed. We are grateful for discussions with Yacine Ait-Sahalia, Michael Fleming, Neil Shephard and comments from Jan Jacobs, Denise Osborn, Andrew Patton and participants at SoFiE, the Cambridge-Princeton Exchange, the Marie-Curie Training Workshop on High Frequency. We also thank Shabir AA Saleem for able research assistance. We are grateful to Ross Adams for managing the database.

Disclosure statement

No potential conflict of interest was reported by the author(s).

Funding

Dungey and Yao acknowledge support from Australian Research Council [grant number DP130100168]. Yalaman acknowledges support from an Eskisehir Osmangazi University Research [grant number 201717A234].

ORCID

Abdullah Yalaman http://orcid.org/0000-0002-4721-6576

References

Aït-Sahalia, Y. and Jacod, J., Estimating the degree of activity of jumps in high frequency data. *Ann. Statist.*, 2009a, **37**(5A), 2202–2244.

Aït-Sahalia, Y. and Jacod, J., Testing for jumps in a discretely observed process. *Ann. Statist.*, 2009b, **37**(1), 184–222.

Aït-Sahalia, Y. and Jacod, J., Is Brownian motion necessary to model high-frequency data? *Ann. Statist.*, 2010, **38**(5), 3093–3128.

Aït-Sahalia, Y. and Jacod, J., Testing whether jumps have finite or infinite activity. *Ann. Statist.*, 2011, **39**(3), 1689–1719.

Aït-Sahalia, Y. and Jacod, J., Analyzing the spectrum of asset returns: Jump and volatility components in high frequency data. *J. Econ. Lit.*, 2012a, **50**(4), 1007–1050.

Aït-Sahalia, Y. and Jacod, J., Identifying the successive Blumenthal-Getoor indices of a discretely observed process. *Ann. Statist.*, 2012b, **40**(3), 1430–1464.

Aït-Sahalia, Y. and Kimmel, R., Maximum likelihood estimation of stochastic volatility models. *J. Financ. Econ.*, 2007, **83**(2), 413–452.

Aït-Sahalia, Y. and Xiu, D., Increased correlation among asset classes: Are volatility or jumps to blame, or both?. *J. Econom.*, 2016, **194**(2), 205–219.

Aït-Sahalia, Y., Cacho-Diaz, J. and Laeven, R.J., Modeling financial contagion using mutually exciting jump processes. *J. Financ. Econ.*, 2015, **117**(3), 585–606.

Akay, O.O., Senyuz, Z. and Yoldas, E., Hedge fund contagion and risk-adjusted returns: A Markov-switching dynamic factor approach. *J. Empir. Finance*, 2013, **22**, 16–29.

Alexeev, V., Dungey, M. and Yao, W., Time-varying continuous and jump betas: The role of firm characteristics and periods of stress. *J. Empir. Finance*, 2017, **40**, 1–19.

Alexeev, V., Urga, G. and Yao, W., Asymmetric jump beta estimation with implications for portfolio risk management. *Int. Rev. Econ. Finance*, 2019, **62**, 20–40.

Andersen, T.G. and Bollerslev, T., Answering the skeptics: Yes, standard volatility models do provide accurate forecasts. *Int. Econ. Rev. (Philadelphia)*, 1998, **39**(4), 885–905.

Andersen, T.G., Bollerslev, T. and Diebold, F.X., Roughing it up: Including jump components in the measurement, modeling, and forecasting of return volatility. *Rev. Econ. Stat.*, 2007, **89**(4), 701–720.

Azzalini, A., A class of distributions which includes the normal ones. *Scand. J. Statist.*, 1985, **12**(2), 171–178.

Bae, K.-H., Karolyi, G.A. and Stulz, R.M., A new approach to measuring financial contagion. *Rev. Financ. Stud.*, 2003, **16**(3), 717–763.

Baur, D. and Schulze, N., Coexceedances in financial markets–a quantile regression analysis of contagion. *Emerg. Markets Rev.*, 2005, **6**(1), 21–43.

Billio, M. and Caporin, M., Market linkages, variance spillovers, and correlation stability: Empirical evidence of financial contagion. *Comput. Stat. Data. Anal.*, 2010, **54**(11), 2443–2458.

Bjursell, J., Wang, G.H.K. and Webb, R.I., Jumps and trading activity in interest rate futures markets: The response to macroeconomic announcements. *Asia-Pac. J. Financ. Stud.*, 2013, **42**(5), 689–723.

Black, A., Chen, J., Gustap, O. and Williams, J.M., The importance of jumps in modelling volatility during the 2008 financial crisis. Technical Report, 2012. Available at SSRN 2118486.

Bollerslev, T., Li, S.Z. and Todorov, V., Roughing up beta: Continuous versus discontinuous betas and the cross section of expected stock returns. *J. Financ. Econ.*, 2016, **120**(3), 464–490.

Bordo, M.D., An historical perspective on the crisis of 2007–2008, Working Paper 14569, National Bureau of Economic Research, 2008.

Bormetti, G., Calcagnile, L.M., Treccani, M., Corsi, F., Marmi, S. and Lillo, F., Modelling systemic price cojumps with Hawkes factor models. *Quant. Finance*, 2015, **15**(7), 1137–1156.

Boyson, N.M., Stahel, C.W. and Stulz, R.M., Hedge fund contagion and liquidity shocks. *J. Finance*, 2010, **65**(5), 1789–1816.

Busetti, F. and Harvey, A., When is a copula constant? a test for changing relationships. *J. Financ. Econom.*, 2011, **9**(1), 106–131.

Calcagnile, L.M., Bormetti, G., Treccani, M., Marmi, S. and Lillo, F., Collective synchronization and high frequency systemic instabilities in financial markets. *Quant. Finance*, 2018, **18**(2), 237–247.

Caporin, M., Pelizzon, L., Ravazzolo, F. and Rigobon, R., Measuring sovereign contagion in Europe. *J. Financ. Stab.*, 2018, **34**, 150–181.

Dungey, M. and Hvozdyk, L., Cojumping: Evidence from the US Treasury bond and futures markets. *J. Bank. Financ.*, 2012, **36**(5), 1563–1575.

Dungey, M., Fry, R., Gonzalez-Hermosillo, B. and Martin, V., Empirical modelling of contagion: A review of methodologies. *Quant. Finance*, 2005, **5**(1), 9–24.

Dungey, M., Fakhrutdinova, L. and Goodhart, C., After-hours trading in equity futures markets. *J. Fut. Markets*, 2009a, **29**(2), 114–136.

Dungey, M., McKenzie, M. and Smith, L.V., Empirical evidence on jumps in the term structure of the US treasury market. *J. Empir. Finance*, 2009b, **16**(3), 430–445.

Dungey, M., Milunovich, G., Thorp, S. and Yang, M., Endogenous crisis dating and contagion using smooth transition structural garch. *J. Bank. Financ.*, 2015, **58**, 71–79.

Dungey, M., Erdemlioglu, D., Matei, M. and Yang, X., Testing for mutually exciting jumps and financial flights in high frequency data. *J. Econom.*, 2018, **202**(1), 18–44.

Dungey, M., Matei, M. and Treepongkaruna, S., Examining stress in Asian currencies: A perspective offered by high frequency financial market data. *J. Int. Financ. Markets Inst. Money*, 2020, **67**, 101200.

Fry, R., Martin, V.L. and Tang, C., A new class of tests of contagion with applications. *J. Bus. Econ. Stat.*, 2010, **28**(3), 423–437.

Jiang, G.J., Lo, I. and Verdelhan, A., Information shocks, liquidity shocks, jumps, and price discovery: Evidence from the U.S. treasury market. *J. Financ. Quant. Anal.*, 2011, **46**(2), 527–551.

Kaminsky, G.L., Reinhart, C.M. and Végh, C.A., The unholy trinity of financial contagion. *J. Econ. Perspect.*, 2003, **17**(4), 51–74.

Lahaye, J., Laurent, S. and Neely, C.J., Jumps, cojumps and macro announcements. *J. Appl. Econom.*, 2011, **26**(6), 893–921.

Li, J., Todorov, V. and Tauchen, G., Jump regressions. *Econometrica*, 2017, **85**(1), 173–195.

Mizrach, B. and Neely, C.J., The transition to electronic communications networks in the secondary treasury market. *Review*, 2006 Nov, **86**(6), 527–542.

Nelson, D.B., Arch models as diffusion approximations. *J. Econom.*, 1990, **45**(1), 7–38.

Pukthuanthong, K. and Roll, R., Internationally correlated jumps. *Rev. Asset Pric. Stud.*, 2015, **5**(1), 92–111.

Rodriguez, J.C., Measuring financial contagion: A copula approach. *J. Empir. Finance*, 2007, **14**(3), 401–423.

Rose, A.K. and Spiegel, M.M., Cross-country causes and consequences of the 2008 crisis: Early warning. *Jpn. World. Econ.*, 2012, **24**(1), 1–16.

Todorov, V. and Tauchen, G., Activity signature functions for high-frequency data analysis. *J. Econom.*, 2010, **154**(2), 125–138.

Yao, W., Dungey, M. and Alexeev, V., Modelling financial contagion using high frequency data. *Econ. Rec.*, 2020, **96**(314), 314–330.